The 2019 Raikoke eruption as a testbed for rapid assessment of volcanic atmospheric impacts by the Volcano Response group

Jean-Paul Vernier[1,2], Thomas J. Aubry[34], Claudia Timmreck[43], Anja Schmidt[5,5b,5c], Lieven Clarisse[6], Fred Prata[7], Nicolas Theys[8], Andy Andrew T. Prata[9,*], Graham Mann[10], Hyundeok Choi[11] , Simon Carn[12], Richard Rigby[13], Susan C. Loughlin[14] and John A. Stevenson[14]

(1) National Institute of Aerospace, Hampton, VA 23692

(2) NASA Langley Research Center, Hampton, VA 23692

(34) Department of Earth and Environmental Sciences, University of Exeter, Penryn, UK

(43) Max-Planck-Institut für Meteorologie, Hamburg, Germany

(5) Institute of Atmospheric Physics (IPA), German Aerospace Center (DLR), Oberpfaffenhofen, German

(5b) Meteorological Institute, Ludwig Maximilian University of Munich, Munich, Germany

(5c) Department of Chemistry, University of Cambridge, Cambridge, United Kingdom

(6) Université libre de Bruxelles (ULB), Service de Chimie Quantique et Photophysique, Atmospheric Spectroscopy, Brussels, Belgium

(7) AIRES Pty Ltd, Mt Eliza, Victoria, Australia

(8) Royal Belgian Institute for Space Aeronomy (BIRA-IASB), Brussels, Belgium

(9) Sub-Department of Atmospheric, Oceanic and Planetary Physics, University of Oxford, Oxford OX1 3PU, UK.

*now at School of Earth, Atmosphere and Environment, Monash University, Clayton, Victoria 3800, Australia.

(10) University of Leeds, Leeds, UK.

(11) Science Applications International Corporation (SAIC), Inc. at NOAA/NWS/NCEP/Environmental Modeling Center, College Park, MD 20740

(12) Michigan Tech, USA

(13) Centre for Environmental Modelling and Computation, School of Earth and Environment, University of Leeds, UK

(14) British Geological Survey, Edinburgh, UK

Correspondence to: Jean-Paul Vernier (jeanpaul.vernier@gmail.com)

Field Code Changed

Formatted: Font: (Default) Times New Roman, English (United States)

Abstract. The 21st June 2019 Raikoke eruption (48°N,153°E) generated one of the largest amounts of sulfur emission to the stratosphere since the 1991 Mt Pinatubo eruption. Satellite measurements indicate a consensus best estimate of 1.5 Tg for the sulfur dioxide (SO_2) injected at an altitude of around 14-15 km. The peak northern hemisphere mean 525nm Stratospheric Aerosol Optical Depth (SAOD) increased to 0.025, a factor of three higher than background levels. The Volcano Response (VolRes) initiative provided a platform for the community to share information about this eruption, which significantly enhanced coordination efforts in the days after the eruption. A multi-platform satellite observation sub-group formed to prepare an initial report to present eruption parameters including SO_2 emissions and their vertical distribution for the modelling community. It allowed to make the first estimate of what would be the peak in SAOD one week after the eruption using a simple volcanic aerosol model. In this retrospective analysis, we show that revised volcanic SO_2 injection profiles yield a higher peak injection of the SO_2 mass. This highlights difficulties in accurately representing the vertical distribution for moderate SO_2 explosive eruptions in the lowermost stratosphere due to limited vertical sensitivity of current satellite sensors (+/- 2 km accuracy) and low horizontal resolution of lidar observations. We also show that the SO_2 lifetime initially assumed in the simple aerosol model was overestimated by 66%, pointing to challenges for simple models to capture how the life cycle of volcanic gases and aerosols depends on the SO_2 injection magnitude, latitude and height. Using revised injection profile, modelling results indicate a peak northern hemisphere monthly mean SAOD at 525nm of 0.024, in excellent agreement with observations, associated with a global monthly mean radiative forcing of -0.17 W/m^2 resulting in an annual global mean surface temperature anomalies of -0.028 K. Given the relatively small magnitude of the forcing, it is unlikely that the surface response can be dissociated from surface temperature variability.

1. Introduction.

After 95 years of dormancy, the Raikoke volcano in the Kuril Islands (North-West Pacific; 48.292°N, 153.25°E) began a series of explosions at 18UTC on 21 June 2019 lasting around 24 hours. Raikoke forms a small uninhabited Island of 2 km x 2.5 km which belongs to the Russian federation, 16 km from Matua Island in the Sea of Okhotsk. Its name originates from the ancient Japanese Ainu language and translate to "hellmouth", referring to past volcanic eruptions. The first eruption reports of Raikoke originated from the mid-18th century but it was during the 1788 eruption that one third of the Island was destroyed (Gorshkov, 1970). The last known eruption was reported in February 1924. Since then, the volcano remained dormant. The volcano is monitored by the Sakhalin Volcanic Eruption Response Team (SVERT), part of the Institute of marine geology and the Kamchatka Volcanic Eruption Response Team (KVERT). During the latest 2019 eruption, the first explosion of a series of 8 was reported by KVERT on 21 June at 17h50 UTC and quickly followed 1h later by a volcanic ash advisory produced by the Tokyo Volcanic Ash Advisory Center (VAAC) responsible to provide ash warnings to the International Civil Aviation Organization (ICAO) across the Pacific Northwest (Sennert, 2019). In addition, KVERT ~~and SVERT issued~~ which issue volcano observatory notice warning for aviation had flagged with an aviation color code red which signifies that an "eruption was underway with significant emission ash into the atmosphere" (see KVERT webpage for more information http://www.kscnet.ru/ivs/kvert/van/index?type=1) ~~red warnings for aviation~~. As a result, nearly 40 flights were re-routed to avoid volcanic ash clouds.

Firstov et al., (2020) analyzed Infrasound Signal (IS) from overpressure measurements from ground stations in Kamchatka and found a total of 11 explosive episodes (see bottom of Fig.1a). The first 8 episodes were followed by a continuous episode (9) which lasted for 3.5 h. Based on IS analysis, episodes are separated into magma fragmentation/ non-stationary processes and vent outflow (1,2,3,7,9 and 10) of ash-gas into the atmosphere. They were used to derive a minimal eruption tephra volume of 0.1 km^3 allowing to categorize the eruption as Volcanic Explosivity Index (VEI) 4 (Firstov et al., 2020). Fig1b shows cloud top temperature (11µm) and associated cloud top heights derived from Himawari-8 geostationary satellite compared with IS data shown in Fig.1a. The eruption started at around 18:00 UTC on 21 June 2019 followed by at least 8 discrete “bursts” (eruptions) and continuous emissions. A further two discrete pulses occurred later. The IS analysis coincides very well with the Himawari-8 observations where each IS corresponds to the release of volcanic cloud into the atmosphere. Muser et al. (2020) used one-dimensional volcanic plume models (Mastin, 2007; Folch et al., 2016) to invert the mass eruption rate of ash and initialize the ICON-ART (Zängl et al., 2015) dispersion model to investigate the complex aerosol, dynamical and radiative processes governing the plume evolution. More simplistic initialization approach with the dispersion model NAME (Beckett et al., 2020) and the aerosol-chemistry-climate model WACCM (Mills et al., 2016) were performed during the VolRes activities shortly after the eruption to assess the early dispersion of the plume.

As part of the scientific response to the eruption, the Volcano Response (Volres) initiative triggered an initial dialogue among the science community. VolRes is an international working group, within the Stratospheric Sulfur and its Role in Climate (SSiRC), to establish co-operation and community planning, for the next large-magnitude eruption, aligned also to the NASA initiative for US-based volcano response plan (Carn et al., 2021). The SSiRC initiative is itself an activity within the SPARC project of the World Climate Research Program (WCRP). Since its inception in 2015, VolRes consist of more than 250 scientists worldwide, from a diverse range of both model and observational experts, aiming to contribute from sharing and discussion of information related to the atmospheric impacts of volcanoes. Discussion and sharing to the mailing list is maintained through an archive and Wiki page, structured by eruption since 2018 (https://wiki.earthdata.nasa.gov/display/volres[a]).

The discussions on the VolRes forum have mostly been focused towards: i) establishing initial estimates of the emitted SO_2 and ash, and injection heights estimates from multiple satellite observation platforms; ii) the expected impacts on stratospheric aerosol loadings; iii) factors to consider in modelling the aerosol cloud, towards then projecting radiative and climate effects; and iv) common related findings after other similar eruptions. Several cross-institutional co-operations resulted from the VolRes activity, which also motivated the Raikoke ACP/AMT/GMD inter-journal special issue “Satellite observations, in situ measurements and model simulations of the 2019 Raikoke eruption “. The Raikoke special issue includes a series of publications (Muser et al., 2020; Kloss et al., 2021; Vaughan et al., 2021; de Leeuw et al., 2021; Horváth et al., 2021a,b; Gorkavyi et al., 2021; Inness et al., 2022; Mingari et al., 2022; Osborne et al., 2022; Bruckert et al., 2022; Capponi et al., 2022; Cai et al., 2022; Harvey et al., 2022; Knepp et al., 2022; Prata et al., 2022; Petracca et al., 2022) focusing on the atmospheric impacts of this eruption using satellite Low Earth Orbiting/Geostationary nadir and limb observations from UV-Visible to far IR, model simulations, airborne measurements and ground-based lidar observations.

The goals of this paper is to:

- Describe the activities undertaken by the Volcano Response group (VolRes, https://wiki.earthdata.nasa.gov/display/volres) at the time of the 2019 Raikoke eruption. A chronology of these activities is provided in Table 1~~2~~.
- Give an overview of the early estimates of the mass of SO_2 emitted as well as the associated radiative forcing and temperature response inferred quickly after the eruption.
- Discuss how revised estimates of SO_2 mass and plume heights as well as radiative forcing estimates differ from the rapid assessment made a week after the eruption.
- Summarize the findings of the Raikoke special issue and highlight the remaining science questions as well as the challenges associated with rapid response to volcanic eruptions in the context of atmospheric impacts.

2. Satellite Datasets

~~HIMAWARI~~Himawari-8

Himwari-8 is a spacecraft developed and operated by the Japanese Meteorological Organization (JAXA). The primary instrument aboard Himawari 8 is the Advanced Himawari Imager (AHI), a 16 multi-channel spectral imager to capture visible light and infrared images of the Asia-Pacific region at 500m horizontal resolution and every 10 minutes. AHI is used to derived the cloud-top temperature and associated cloud top height associated with the Raikoke eruption.

TROPOMI

The TROPOspheric Monitoring Instrument (TROPOMI), on-board the Sentinel-5 Precursor satellite, provides atmospheric composition measurements (Veefkind et al., 2012) at high spatial resolution of 3.5 x 5.5 km². TROPOMI is a hyperspectral sounder with different spectral bands from the ultraviolet (UV) to the short-wave infrared. TROPOMI provides nearly global coverage in one day at 1.30 pm local time. For a rapid assessment of the total emitted SO_2 mass, the operational SO_2 product (Theys et al., 2017) was used. A refined analysis was then performed with the scientific SO_2 layer height and vertical column joint retrieval of Theys et al.(2022)

IASI

The Infrared Atmospheric Sounding Interferometer (IASI) is the high spectral resolution infrared sounder onboard the operational Metop A-B-C platforms. With a morning and evening overpass (around 9:30 AM and PM), combined with a large swath, the instrument samples the entire globe twice a day. Its footprint is a 12km diameter circle at nadir viewing angles, gradually increasing to a 20 km x 39 km ellipse at the far end of its swath. The SO_2 product that was used for rapid assessment is the one detailed in Clarisse et al. (2014). The retrieval algorithm consists of two steps. First a so-called Z function that is estimated for each observed spectrum, using a set of derivatives (Jacobians) with respect to the SO_2 partial columns at varying altitudes. The altitude at which Z function reaches is maximum is the retrieved SO_2 height. In a second step, the estimated SO_2 height is used to constrain the IASI SO_2 column retrieval. Note that the entire retrieval uses the 7.3 µm absorption band of SO_2, which is less affected by ash than the 8.6 µm band. While the altitude algorithm has a general accuracy better than 2 km, it is known to underestimate the SO_2 altitude for high SO_2 columns. For the refined analysis discussed below, a new experimental product was used that deals better with saturation issues.

Aqua/AIRS

The atmospheric Infrared Radiation Sounder (AIRS) instrument is on-board the NASA polar-orbiting Aqua satellite at an altitude of about 705 km above the Earth surface with an eEquatorial crossing time at 1.30am/pm local time (Chahine et al., 2005; Prata & Bernardo, 2007). AIRS provides nearly continuous measurement coverage during 14.5 orbits per day and a 95% global daily coverage with a swath of 1650 km and special resolution of 13.5 km x 13.5 km at nadir (Tournigand et al., 2020). We use the version 7.0 AIRS level 2 Support Retrieval product, and the results are averaged into 1° x 1° grid cells in this analysis. The Bbrightness Ttemperature Ddifference (BTD, less than -6 K) is used as a proxy of SO_2 released from volcanoes. For more information about the AIRS BTD, see https://docserver.gesdisc.eosdis.nasa.gov/public/project/AIRS/V7_L2_Product_User_Guide.pdf (p102-103).

CALIPSO/CALIOP

The Cloud-Aerosol Lidar with Orthogonal Polarization (CALIOP), on-board the Cloud-Aerosol Lidar and Infrared Pathfinder Satellite Observations (CALIPSO) platform, has been providing aerosol vertical profile measurements of the Earth's atmosphere on a global scale since June 2006 (Winker et al., 2010). We use the version 4.21 CALIOP level 2 Aerosol layer and Cloud layer products, and only quality screened samples are used in the analysis. The Cloud Aerosol Discrimination (CAD) is the algorithm that evaluates CALIOP observables to classify layers and assign values between -100 (certainly aerosol) and 100 (certainly cloud). Aerosol layers with CAD score less than -100 or greater than -20 are rejected to avoid low confidence (Winker et al., 2013; Tackett et al., 2018). Aerosol layers with the extinction Quality Control (QC) flag that are not equal to 0, 1, 16, and 18 are rejected to remove low confidence extinction retrievals. Detailed information of the QC flag can be found in Tackett et al. (2018). In addition, aerosol extinction samples with the extinction uncertainty equal to 99.99 km^{-1} and all samples at lower altitudes in the profile are rejected to remove unreliable extinctions (Winker et al., 2013).

Firstov et al., (2020) analyzed Infrasound Signal (IS) from ground stations in Kamchatka and found a total of 11 explosive episodes (see Fig.1a). The first 8 episodes were followed by a continuous episode (9) which lasted for 3.5 h. Based on IS analysis, episodes are separated into magma fragmentation/ non-stationary processes and vent outflow (1,2,3,7,9 and 10) of ash-gas into the atmosphere. They were used to derive a minimal eruption tephra volume of 0.1 km^3 allowing to categorize the eruption as Volcanic Explosivity Index (VEI) 4 (Firstov et al., 2020). Fig1b shows cloud top temperature (11µm) and associated cloud top heights derived from Himawari-8 geostationary satellite compared with IS data shown in Fig.1a. The eruption started at around 18:00 UTC on 21 June 2019 followed by at least 8 discrete "bursts" (eruptions) and continuous emissions. A further two discrete pulses occurred

Formatted: Font: (Default) Times New Roman, 10 pt, English (United States)

~~later. The IS analysis coincides very well with the Himawari-8 observations where each IS corresponds to the release of volcanic cloud into the atmosphere. Muser et al. (2020) used one-dimensional volcanic plume models (Mastin, 2007; Folch et al., 2016) to invert the mass eruption rate of ash and initialize the ICON-ART dispersion model to investigate the complex aerosol, dynamical and radiative processes governing the plume evolution. More simplistic initialization approach with the dispersion model NAME and the aerosol-chemistry-climate model WACCM were performed during the VolRes activities shortly after the eruption to assess the early dispersion of the plume.~~

~~4~~3. Early reports of injection parameters one week after the eruption

One of the main activities of a satellite sub~~-~~group formed within the framework of VolRes was to derive eruption parameters characterizing SO_2 emissions (e.g. mass, bulk height, injection profiles) as soon as possible so that modelers would run numerical simulations to understand the potential hazards and climate impacts of this eruption. The basic approach to estimate the total mass of SO_2 is similar for each satellite-based sensor. First, the process involves retrieving the Vertical Column Density (VDC, measured in molecules cm^{-2} or g m^{-2} or Dobson units) in each pixel affected by SO_2, followed by multiplying by the area of the pixels and integrating all the pixels to calculate the total SO_2 loadings. However, there are limitations to this method. Indeed, narrow swath width sensors, timing of the polar orbit and, in the case of the geostationary sensors, extreme viewing geometry (high satellite zenith angles) and movement out of the field of view will introduce errors (likely underestimations) of the total mass. There are also many assumptions used by the various algorithms that if not valid will introduce errors, as will be discussed hereunder. When the Vertical Column Densities (VCDs) are large (>500 DU) most algorithms have difficulty estimating the VCD correctly (Hyman and Pavolonis, 2020; Prata et al. 2021).

Figure 2 shows the time evolution of the total SO_2 mass during and after the Raikoke eruption from multiple sensors. The measurements discussed here all assume SO_2 in the UTLS (7–12 km). The SO_2 retrieved from Himawari-8 peaks near 1.5 Tg nearly 48h after the beginning of the eruption and follow similar temporal evolution ~~than~~ as the one derived from Low Earth Orbit (LEO) satellites ~~EO~~. Given the likelihood that most satellites underestimated the SO_2 mass, we chose at that time the maximum value from Himawari and the upper limits of the other sensors yielding a 1.5+/-0.2 Tg estimation. IASI, TROPOMI and CALIPSO data suggested that SO_2 was injected within a large altitude range from the ground up to well in the stratosphere (at least 15 km). In addition to a total mass of SO_2 (of 1.5 Tg), the VolRes team also issued a provisional vertical distribution of the emitted SO_2 mass that could be used by dispersion and climate modelers. To do so, IASI SO_2 height measurements on the 22[nd] June 2019 were used. The mass-altitude indicated that most SO_2 was released between 8-12 km with a secondary peak around 14-15 km. Scaled to the proposed 1.5 Tg, the distribution is shown in Figure 3 and is referred to as the 'VolRes profile' (blue line; also see Table 2~~1~~). For TROPOMI, and other LEOs, the plume can be partly covered by a given orbit but using the multiple orbits of one day and the fact that they generally overlap most of the plume is covered. To avoid double counting, the data of one full day are usually averaged on a regular latitude-longitude grid, before the actual emitted SO_2 mass is calculated. An important source of error is the vertical distribution of SO_2. In

Fig.2, the retrieved SO_2 mass from TROPOMI was calculated by assuming a bulk plume height of 15 km (all plume heights given above sea level unless specified). This assumption can introduce errors (underestimation) in particular for clear-sky scenes and if the SO_2 is in the (lower) troposphere, typically below 7km, see e.g., Fig 1 of Theys et al. (2013). TROPOMI has less limitations in retrieving very large SO_2 columns (>500 DU) because in that case the spectral range used (360-390nm) is weakly affected by saturation due to non-linear SO_2 absorption (Bobrowski et al., 2010). The main problem is the presence of aerosols which are not explicitly treated in the retrievals (Theys et al., 2017). For ash, the photons cannot penetrate deep in the volcanic cloud (only the cloud top layer is sensed) and this leads to a strong underestimation of the mass of SO_2 (by a factor of 5 or so).

~~5~~4. Revision and improvements of injection parameters.

While the accuracy of the IASI SO_2 height retrievals is typically better than 2km, it became clear however that the VolRes profile was peaking too low in the atmosphere (e.g., de Leeuw et al., 2021). The main reason for this is related to the SO_2 Jacobeans used in the retrieval. These are precalculated for relatively low SO_2 VCDs and are not directly applicable to saturated plumes, as encountered during the Raikoke eruption. Refinement of the IASI algorithm to better account for this dependence on the SO_2 loadings has led to SO_2 injection profile with a maximum SO_2 peaking at ~14-15 km (see Figure 3) and a slightly lower total mass of ~1.3 Tg SO_2 (even though total mass estimates for the days after reach again 1.5 Tg and higher).

As an alternative to IASI, ultraviolet observations from the TROPOMI nadir sensor have been used to estimate the SO_2 injection profile (Table 2~~1~~). Conceptually, the retrieval algorithm is like the IASI scheme. It relies on an iterative approach making use of a SO_2 optical depth look-up-table, where both SO_2 height and vertical column are retrieved jointly (Theys et al., 2021). The accuracy of the retrieved SO_2 heights is of 1-2 km, except when coincident with fresh and optically thick ash plumes for which the estimated heights can be strongly biased low. Because of this, the first reliable profile from TROPOMI which covers the full plume, is for the 24 June 2019. The maximum SO_2 height is found at ~11-12 km (Figure 3) and the total mass derived is of ~1.2 Tg SO_2. However, the total mass is likely underestimated because only the pixels with confident SO_2 height retrievals are considered (typically for SO_2 columns > 5DU). Selected examples of retrieved SO_2 heights from the two instruments are illustrated in Figure 4.

Although the estimated SO_2 mass from IASI and TROPOMI agree well, the estimated SO_2 profiles show rather inconsistent results with a discrepancy of about 3km for the SO_2 ~~bulk height~~center of mass. It should be emphasized that SO_2 height retrieval from nadir sensors is challenging in general but for Raikoke in particular. The retrievals and their interpretation might also suffer from different aspects. For instance, the UTLS was characterized by isothermal temperature profiles, which can lead to errors on the IASI height estimates. In addition, the measurement sensitivity is different in the ultraviolet than in the thermal infrared and depends on the way the photons interact with the volcanic cloud (and the constituents other than SO_2). In this respect, the retrieved SO_2 heights must be considered as effective heights. Moreover, few CALIOP observations were available (see Section 6) for evaluating the results for the early stage of the eruption.

Despite these challenges, our injection profiles estimates are not in contradiction with results found in the literature:

- Kloss et al. (2021) reported a 14 km altitude plume height based on an early OMPS aerosol extinction profile, on 22 June 2019.
- Muser et al. (2020) derived typical altitudes of 8-14 km from MODIS and VIIRS cloud top height retrievals.
- By slightly adapting (assuming higher injection heights) the VolRes profile, de Leeuw et al. (2021) found the best match between modeled and TROPOMI SO_2 columns for an injection profile with most of SO_2 between 11 and 14 km.
- Hedelt et al. (2019) reported SO_2 heights similar to the TROPOMI results shown here, i.e., with the bulk height below 13km.
- SO_2 height retrievals from the Cross-track Infrared Sounder (CrIS) instrument (Hyman & Pavolonis, 2020) are consistent with plume heights as high as 14-17 km in the plume center, but also show that most of the SO_2 mass was emitted under 13 km.
- Geometric estimation of Raikoke ash column height suggests injection mainly between 5 and 14 km and an overshooting cloud up to 17 km (Horváth et al., 2021b).
- MLS data for 23-27 June indicates SO_2 plumes at 11 to 18 km with maximum columns observed around 14 km (Gorkavyi et al., 2021).
- Using a Langragian transport model combined with TROPOMI and AIRS, Cai et al. (2022) reconstruct an emission profile with a peak at 11 km with a large spread from 6 to 14 km.
- Prata et al. (2022) found ash clouds at a maximum height of 14.2 km (median height of 10.7 ± 1.2 km) during the main explosive phase.

~~6~~5. New plume injection analysis derived from CALIPSO and AIRS

CALIPSO observations were made publicly available within 24-48 h after the beginning of the eruption, allowing accurate early estimates of the height of downwind plume sections. However, due to the narrow swath of the lidar (a few hundred meters) and consequently low ~~horizontal~~ spatial ~~resolution~~coverage, they may not completely represent the entire plume vertical distribution. Nevertheless, an overpass of the CALIPSO lidar across the plume on 22 June 2019 at 2.15 am, ~600 km east from the volcano within an SO_2 cloud observed by OMPS show volcanic layers between 9-13.5 km (Prata et al., 2021). A second overpass the next day depicts another volcanic layer between 15-16 km. Those observations were used to validate SO_2 emission profiles provided to the community a week after the eruption. Here, we give a more comprehensive analysis of the plume injection height using a combination of quasi-collocated (less than 1h apart) SO_2 observations from AIRS and detected volcanic layers from CALIOP during the first two weeks after the eruption. The brightness temperature difference (1361.44-1433.06 cm^{-1}) is used as a proxy of SO_2 released from volcanoes to identify CALIOP data within the SO_2 plume.

We combined SO_2 information from AIRS quasi-collocated observations from CALIOP to further investigate plume injection heights after the Raikoke eruption assuming that SO_2 and volcanic aerosols remained collocated in space and time during the first 10 days after the eruption. Figure 5a shows a map of SO_2 derived from AIRS together with CALIOP orbit tracks (red). The corresponding cloud and aerosol level 2 V4.2 products are plotted along with BTD extracted along the orbit (Fig.5b). All corresponding layers (clouds and aerosols) associated with negative BTD

(BTD<6 K, red line Fig5c), indicating the presence of SO_2 in the atmospheric column, have been further analyzed to distinguish the volcanic plume. The distinction is based on the diagram of depolarization and color ratio shown in panel d. Figure 5a shows that CALIOP intersected the plume along two orbit tracks on 25 June. The first being along the 17h53 UTC orbit near 60°N and at two occasions between 55°N-65°N along the third~~second~~ orbit (from the left) near 14h36 UTC. The first intersection (numbered 1) shows the plume near 9-11 km with weak particulate DePolarization Ratio (DPR) (DPR < 0.2) and particulate CoLor Ratio (CLR) near 0.5. DPR values suggest a mixture of ash and sulfate aerosols. However, the second set of intersections (numbered 2 and 3) of the plume shows higher DPR near 0.3 and the same CLR than the first indicating a higher fraction of ash particles resulting in increased DPR values. During those observations, two distinct plumes are visible,~~ between~~ the northern intersection near 11-13 km (green color on diagrams) and a piece at higher altitude (13-15 km) further south (<60°N).

We visually inspected all CALIOP observations (day and night) between 06/22 and 07/06 following the same approach and used plume identification criterion when DPR < 0.4 and CLR < 0.7 and altitude > 5 km to remove tropospheric aerosols and ice clouds. Because of the enhanced noise of the daytime observations, we chose to focus this analysis on nighttime data only. Figure 6 shows the daily observations of the Raikoke plume since the eruption and during the following two weeks. We note that the plume was observed by CALIOP from 8 km to 17 km. The cumulative Probability Density Function (pdf) suggests two main peaks, one near 10-11km km and another smoother peak near 13-15 km. The overall aerosol vertical distribution is consistent with the distribution of SO_2 profiles derived with different approaches and instruments just after the eruption (Fig.3). However, the pdf does not suggest a pronounced peak at a given altitude but rather a flatter distribution as opposed to what is shown in Figure 3. The pdf does not account for or is not weighted by the aerosol loading, which may explain why we do not see a pronounced peak as for the SO_2 profiles derived from IASI and TROPOMI. In addition, SO_2 and volcanic aerosol layers are assumed to be collocated but it may not always be the case.

~~7~~6. Rapid projections of the aerosol forcing and the global mean surface temperature response.

In the previous sections, we discussed in detail the methods used to derive injection parameters (SO_2 total mass, plume heights and SO_2 distribution) which served as input to estimate the radiative and surface temperature responses from the eruption in this section. Key metrics characterizing the climate effects of volcanic eruptions are the peak global mean mid-visible SAOD, the global mean net radiative forcing and the global mean surface temperature change. One motivation of the VolRes initiative is to provide an estimated magnitude for each of these metrics. In the case of a large-magnitude eruption, these initial indicators of the scale of the climate response would then help to determine whether resources should be directed towards additional measurement campaign and the forcing datasets enable the community to run seasonal and decadal forecasts. ~~(Müller and Smith, 2018).~~

The first estimates of the injected SO_2 mass and height became available 24-48 hours after the 2019 Raikoke eruption, followed one week later by an estimate of global mean peak SAOD (7.1), radiative forcing (7.2) and surface temperature (7. 3). This section discusses: i) how these estimates were made; ii) how they compared to observations; and iii) ongoing improvements to the protocol for rapid projection of volcanic forcing and climate impact.

~~7~~6.1 Model simulations of aerosol optical properties

We first made projections for SAOD on 25 June 2019 using EVA_H (Aubry et al., 2020), a simple volcanic aerosol model based on inputs of the mass of volcanic SO_2 injected, its injection height, and the latitude of an eruption. The first estimates made following Raikoke used a range of injection heights between 10-20 km, and a range of the mass of SO_2 of 1-2 Tg of SO_2, on the basis of first estimates of 14 km and 1.5 Tg of SO_2 that initially circulated on the VolRes mailing list (personal communication from "Taha Ghassan" and "Lieven Clarisse"). The corresponding simulated range in peak Northern Hemisphere (25ºN-90ºN, NH) monthly-mean SAOD at 525nm ($SAOD_{525}$) was 0.015-0.023 (Figure 7). This range was obtained using Monte Carlo methods, i.e. EVA_H was run thousands of times, randomly resampling the range of injection height and mass. The negligible computational cost of simple models like EVA_H is a key advantage for providing estimate of the volcanic SAOD perturbation and its uncertainties as soon as measurements of the SO_2 mass and its injection height become available. The SAOD perturbation was projected to be largely confined to 25-90ºN (Figure 8). SAOD perturbations observed in the tropics and Southern Hemisphere over 2019-2020 (Figure 8) are primarily driven by stratospheric emissions from the Ulawun 2019 eruptions and the Australian 2019-2020 wildfires (Kloss et al., 2021).

Following the communication of the initial VolRes SO_2 profile (Figure 3) through the VolRes mailing list, EVA_H peak NH monthly-mean $SAOD_{525}$ estimate for Raikoke were revised to an even smaller value of 0.014. Compared to observations from GloSSAC (v2.1) (Kovilakam et al., 2020), this value was largely underestimated as GloSSAC NH monthly-mean $SAOD_{525}$ peaks at 0.025 (Figure 7, with GloSSAC in excellent agreement with observational values from Kloss et al., 2021) using OMPS-limb data. The new IASI June 22 profile presented in Figure 3 results in a higher peak NH monthly-mean $SAOD_{525}$ of 0.0175, with the higher proportion of stratospheric SO_2 in the new profile more than compensating for the total mass decreasing from 1.5 to 1.29 (average of the two IASI profiles) Tg of SO_2. Although the new SO_2 emission profile improves agreement with observations, the estimated $SAOD_{525}$ value is still a substantial underestimate. Furthermore, the characteristic rise and decay timescales of the $SAOD_{525}$ perturbation are also overestimated by EVA_H (Figure 7). These mismatches are caused by the constant timescale EVA_H uses for SO_2 to sulfate aerosol conversion, which is biased towards an 8-month value adequate for the Pinatubo 1991 eruption (Aubry et al, 2020). If we decrease the value of this timescale by 66% to 2.8 month in EVA_H, the NH peak SAOD value as well as the characteristic rise and decay timescale of the SAOD perturbation are in excellent agreement with observations for the 2019 Raikoke eruption (Figure 7). The fact that this model timescale is independent of the eruption characteristic is an already identified weakness of EVA_H that will be addressed in future developments (Aubry et al., 2020). This timescale has indeed been shown to depend on the volcanic SO_2 mass (e.g. McKeen et al., 1984; Carn et al, 2016), injection altitude and latitude (e.g. Carn et al, 2016, Marshall et al. 2019) as well as co-emission of water vapor (Legrande et al., 2016) and volcanic ash (Zhu et al., 2022).

~~7~~6.2 Projection for global mean volcanic forcing

On the same day that SAOD projections were initially provided, Piers Forster independently suggested via the VolRes mailing list (Forster, personal communication) that the global annual-mean net radiative forcing would be at most -0.2 W m^{-2} (Figure 9, left) based on a scaling between the estimated SO_2 mass of 1.5 Tg SO_2 for 2019 Raikoke and the estimated 15-20 Tg SO_2 for the 1991 Mt. Pinatubo eruption, which resulted in a global annual-mean forcing of -3.2 W/m^2 in 1992. This projection was a back-of-the-envelope calculation using simple proportionality arguments and it did not rely on any SAOD estimates. A monthly global mean peak shortwave forcing with a range from −0.16 to −0.11W/m^2 was derived from SAGE III observations (Kloss et al., 2021). The corresponding annual mean net forcing is expected to be much smaller because of the difference between the peak monthly NH mean SAOD and its average value over the first post-eruption year (Figure 7), as well as the fact that longwave stratospheric volcanic aerosol forcing can offset as much as half of the shortwave forcing (Schmidt et al. 2018). Altogether, the educated guess made for global annual mean radiative forcing was thus likely overestimated.

~~7~~6.3 Projection of the global mean surface temperature response

Last, as part of the eruption response, one day after the first global annual-mean radiative forcing estimate of 0.2 W m^{-2} was made using proportionality arguments and Pinatubo measurements (section 6.2 and Figure 9, left), we estimated that the peak global annual-mean surface temperature change would be -0.02 K (Figure 9, right). We obtained this estimate using FaIR, a simple climate model (Smith et al., 2018). Like EVA_H, FaIR has a negligible computational cost enabling rapid estimates of global-mean surface temperature change following an eruption and facilitating uncertainty estimation, although the latter was not done for the 2019 Raikoke eruption. The model-projected surface temperature response cannot be compared to measurements owing to difficulties in disentangling such a small forced temperature response from temperature variations related to natural variability.

~~8~~7. Discussions

The Raikoke eruption ended a period without moderate volcanic eruptions in the Northern Hemisphere since Nabro in 2011 (Bourassa et al., 2013, Fairlie et al., 2014; Sawamura et al., 2012) which injected 1.5-2 Tg of SO_2 partially distributed between the troposphere and stratosphere. Following the Nabro eruption, the role deep convection during the Summer Asian Monsoon was evoked to explain an apparent ascent of the plume (Bourassa et al., 2013) debated by others (Fromm et al., 2013, Vernier et al., 2013) based on initial observations of injection heights. The substantial debate provoked by this eruption clearly demonstrated the complexity of assessing accurately SO_2 injection heights and their partition relative to the tropopause. The VolRes initiative substantially helps fill those gaps by providing a coordinated structure to derive injection parameters after the Raikoke eruption. Multiple sensors were used to assess the total SO_2 mass and its distribution just one week after the eruption (Fig.3). However, the lack of vertically resolved SO_2 information remains a limitation to accurately assess SO_2 plume distribution and the revised estimates proposed here remain with a 2 km uncertainty regarding the exact position of the plume peak while the initial 1.5 Tg SO_2 mass estimate might be slightly overestimated. Advances in measuring SO_2 with lidar observations may fill those gaps in the future.

The VolRes team provided eruptive parameters within a week after the eruption that strongly helped modelers to estimate climate response of the Raikoke eruption. The use of simple models like EVA_H and FaIR to project the climate response to an eruption in almost near real-time is a powerful way to generate first-order estimates of the perturbations to SAOD, and surface temperatures. Unlike simple proportionality arguments based on the Pinatubo 1991 eruption, these models can estimate the time (and spatial, for EVA_H) evolution of the response variable, and they account for complexities such as the dependency of SAOD on the SO_2 injection latitude and height. Their computationally inexpensive nature also enables a comprehensive quantification of uncertainties related to eruption source parameters, which are often poorly constrained in the days-months following an eruption as highlighted by this special issue, as well as uncertainties on parameters of these empirical models, such as the SO_2-aerosol conversion timescale in EVA_H (Figure 7).

One limitation of the application of these models following the Raikoke 2019 event is that they were not applied in concordance, i.e. FaIR was run using an expert guess for the radiative forcing instead of values derived from EVA_H's SAOD estimates (see section 7.2 and 7.3). Following the Raikoke 2019 VolRes response, we combined the simple models EVA_H (for aerosol forcing) and FaIR (for surface temperature response). To do so, we apply simple linear (Schmidt et al., 2018) or exponential (Marshall et al., 2020) relationships to derive the global mean radiative forcing (FaIR's key input) from the global mean SAOD (one of EVA_H's outputs). EVA_H, SAOD-radiative forcing scalings, and FaIR were for example applied in concordance to estimate the climate impacts from the sulfate aerosols of the January 2022 Hunga Tonga-Hunga Ha'apai eruption. These models have been combined into a single dedicated webtool called Volc2Clim (Schmidt et al., 2023), publicly available at https://volc2clim.bgs.ac.uk/. Applied to Raikoke 2019 using the new injection profile (Figure 3) and revised SO_2 to sulfate aerosol conversion timescale, the beta version of Volc2Clim projected peak global mean of 0.008, -0.17 W/m^2 and -0.028 K for monthly mean SAOD, monthly mean radiative forcing and annual mean temperature anomaly. In addition to key metrics discussed in this section such as global mean SAOD, radiative forcing and surface temperature, aerosol optical properties field (dependent on latitude, altitude and wavelength) are outputted by Volc2Clim for use in climate models that do not have an interactive stratospheric aerosol scheme. With a webtool for rapid estimation of the global climate response during an eruptive crisis, we hope to support communication amongst the scientific community (including VolRes), with authorities and with the public, which in turn will help to mitigate potential consequences arising from the climate effects of an eruption.

Although Volc2Clim offers new perspectives for rapid response and communication following volcanic eruptions, the simplified nature of the models at its core means their result should be considered carefully. As an example, EVA_H currently directly scales the global mean aerosol effective radius from the total mass of aerosol (Aubry et al., 2020). Even for the 1991 Pinatubo eruption, the aerosol effective radius time evolution lagged that of the total mass (e.g. Toohey et al., 2016). Furthermore, Wrana et al. (2023) show that some eruptions injecting less than 1 Tg SO_2 into the stratosphere lead to a reduction of aerosol size, a response opposite to that predicted by EVA_H and thus Volc2Clim. Beyond volcanic sulfate aerosol, Volc2Clim currently does not allow projections of effects related to co-emission of species such as water vapor or halogen in volcanic plumes, or PyroCumulonimbus (PyroCbs) plumes. Before and after the Raikoke eruption, three significant events affected stratospheric aerosols. Indeed, SO_2 injected from the June an August 2019 Ulawun eruptions and smoke from PyroCbs in Canada made the Raikoke eruption even more challenging to understand. The PyroCbs in Canada produced smoke in the UTLS one week

Formatted: Subscript

before the eruption, but the transport patterns of smoke and volcanic aerosols have been distinct (Osborne et al., 2022) and the likelihood for both plumes to mix is relatively small. The Ulawun eruption injected SO_2 which remained relatively confined in the Southern Hemisphere, but we cannot rule out that both plumes got mixed in the tropics (Kloss et al., 2021). The relatively small amount of SO_2 injected by Ulawun (< 0.1 Tg) was not considered in the estimates provided in this paper. Another interesting feature observed after the Raikoke eruption was the formation of a distinct plume which rose into the stratosphere. The plume formed a vortex circulation which remained coherent for several weeks (Gorkavyi et al., 2021) rising in the stratosphere of 10 km over the course of 2-3 months. While this plume shared similar optical properties to smoke, Knepp et al. (2022) concluded that this layer was mostly composed of large sulfuric acid droplets but did not refute the possible presence of a fine ash component. More recently (Khaykin et al, 2023) found that 24% of the total SO_2 mass was contained in the volcanic vortex with a confined anticyclonic circulation detected by wind doppler lidar from Aeolus. A warm anomaly of 1 K was also evident GPS RO Cosmic data demonstrating that the heating of the plume was indeed responsible for its internal circulation and maintenance. Moreover, the properties of the plume observed by CALIOP showed the persistence of ash that likely induced internal heating in the plume consistent with earlier observations of volcanic clouds after the Kelud and Puyehue-Cordon eruptions (Jensen et al., 2018; Vernier et al., 2013, 2016). While the presence of fine ash in the Raikoke could likely explained the maintenance of the vortex as observed after PyroCbs events but with a much faster ascent rate, the interplay between ash and sulfate and influence on radiative calculations is still not understood (Vernier et al., 2016; Stenchikov et al., 2021; Zhu et al., 2020). In addition, we cannot fully rule out that remnants of smoke from the PyroCbs in Canada one week before the eruption could have played a role in the transport of the plume. The increased lifetime of this plume may have produced a larger climate impact than expected since this effect is not included in the simple model provided in this paper (Figure 8). Besides, we cannot rule out that the lower plume lifetime maybe have been affected and influenced by wildfires from Siberia during the summer 2019 as suggested by Ohneiser et al. (2021).

Finally, the recent eruption of Hunga Tonga Hunga Ha'apai (HTHH) demonstrated that sub-marine eruption can inject significant amount of H_2O in the stratosphere (Milan et al., 2022, Vogel et al., 2022; Sellitto et al., 2022) which is known to have oppositive cooling climate effects than sulfate aerosol. The water vapor can reduce the lifetime of SO_2 by providing OH radicals and affect aerosol size distribution through condensational growth (Zhu et al., 2022). Such effects are not included in the simple climate estimates provided here and would limit its applicability in the case of HTHH if only the climate impacts of sulfate aerosols are considered.

~~9~~8. Conclusion

VolRes is an international coordinated initiative to study the atmospheric impacts of volcanic eruptions, now involving more than 250 researchers worldwide. The 2019 Raikoke eruption triggered significant responses by the VolRes community through exchanges of information via the mailing list and the preparation of SO_2 profile recommendations for modelers made available a week after the eruption only. Our paper gives a brief overview of how the community responded to this volcanic eruption, which is documented extensively in the Raikoke special issue. We then described how early estimates of SO_2 emission and height, a fundamental parameter which dictates the plume lifetime and its impacts, were derived from satellite observations. These estimates were used by VolRes to calculate SAOD, radiative forcings and surface temperature changes as part of the initial eruption response. We revisited the initial SO_2 injection profiles by addressing saturation effects due to high SO_2 column density to improve plume injection heights. We highlight remaining challenges in accurately representing the vertical distribution for moderate- SO_2 explosive eruptions in the lowermost stratosphere due to limited vertical sensitivity of current satellite sensors (+/- 2 km accuracy) and low horizontal resolution of lidar observations. We found that using revisited SO_2 injection heights and reduced SO_2-aerosol conversion timescale in a simple volcanic aerosol model (EVA_H) improves SAOD estimates relative to available observations from the GloSSAC dataset. The protocol for fast estimation of aerosol optical properties, radiative forcing and surface temperature response to volcanic eruption has since been implemented in a seamless webtool (Volc2Clim, https://volc2clim.bgs.ac.uk/). The computationally inexpensive nature of the webtool makes it ideal for rapid assessment of the volcanic climate effect and for propagating large uncertainties that characterize early observations of volcanic clouds. Further development of the underlying simple models as well as continued use of complex models explicitly modelling aerosol chemistry, microphysics and transport remain critical given the complex nature of volcanic events. For example, the Raikoke eruption took place in connection with two eruptions of Ulawun in June and August 2019 and just after a PyroCb event which transported smoke into the stratosphere which were not considered in our original or revised calculations. In addition, the recent HTHH eruption demonstrated that water vapor can also be injected into the stratosphere which can affect SO_2 and aerosol lifetime but also with a radiative forcing that is opposite to volcanic sulfate aerosols.

Competing interests

The contact author has declared that none of the authors has any competing interests.

Acknowledgement.

JPV and HC were supported by the NASA Roses program through the SAGE III Science Team (80NSSC21K1195) and Upper Atmosphere Composition Observations program (80NSSC21K1082). TJA was supported by a global mobility grant from the University of Exeter and a travel award from the Canada-UK foundation. CT acknowledges support for this research by the Deutsche Forschungsgemeinschaft Research Unit VolImpact (FOR2820,398006378) within the project VolClim (TI 344/2-1). ATP acknowledges funding from the Natural Environment Research Council (NERC) R4Ash project (NE/S003843/1). The Volc2Clim tool was kindly supported by the UK Earth System Modelling project, funded by the UKRI – Natural Environment Research Council (NERC) national capability grant number NE/N017951/1 and the Met Office, as well as NERC grants NE/S000887/1 (VOL-CLIM) and NE/S00436X/1 (V-PLUS). The GloSSAC data were obtained from the NASA Langley Research Center Atmospheric Sciences Data Center. The Volc2Clim webtool is available at https://volc2clim.bgs.ac.uk/, and the source code is available on GitHub at https://github.com/cemac/volc2clim/. The source code of the EVA_H volcanic aerosol model is available on GitHub at https://github.com/thomasaubry/EVA_H. The source code of the FaIR climate model is available on Github at https://github.com/OMS-NetZero/FAIR.

References:

Aubry, T. J., Toohey, M., Marshall, L., Schmidt, A., & Jellinek, A. M. (2020). A New Volcanic Stratospheric Sulfate Aerosol Forcing Emulator (EVA_H): Comparison With Interactive Stratospheric Aerosol Models. *Journal of Geophysical Research: Atmospheres*, *125*(3), e2019JD031303. https://doi.org/https://doi.org/10.1029/2019JD031303

Beckett, Frances M., et al. "Atmospheric dispersion modelling at the London VAAC: A review of developments since the 2010 eyjafjallajökull volcano ash cloud." Atmosphere 11.4 (2020): 352.

Bobrowski, N., Kern, C., Platt, U., Hörmann, C., & Wagner, T. (2010). Novel SO_2 spectral evaluation scheme using the 360–390 nm wavelength range. *Atmospheric Measurement Techniques*, *3*(4), 879–891. https://doi.org/10.5194/amt-3-879-2010

Bourassa, A. E., Robock, A., Randel, W. J., Deshler, T., Rieger, L. A., Lloyd, N. D., Llewellyn, E. J. (Ted), & Degenstein, D. A. (2012). Large Volcanic Aerosol Load in the Stratosphere Linked to Asian Monsoon Transport. *Science*, *337*(6090), 78–81. https://doi.org/10.1126/science.1219371

Bruckert, J., Hoshyaripour, G. A., Horváth, Á., Muser, L. O., Prata, F. J., Hoose, C., and Vogel, B.: Online treatment of eruption dynamics improves the volcanic ash and SO_2 dispersion forecast: case of the 2019 Raikoke eruption, Atmos. Chem. Phys., 22, 3535–3552, https://doi.org/10.5194/acp-22-3535-2022, 2022.

Cai, Z., Griessbach, S., & Hoffmann, L. (2022). Improved estimation of volcanic SO_2 injections from satellite retrievals and Lagrangian transport simulations: the 2019 Raikoke eruption. *Atmospheric Chemistry and Physics*, *22*(10), 6787–6809. https://doi.org/10.5194/acp-22-6787-2022

Capponi, A., Harvey, N. J., Dacre, H. F., Beven, K., Saint, C., Wells, C., and James, M. R.: Refining an ensemble of volcanic ash forecasts using satellite retrievals: Raikoke 2019, Atmos. Chem. Phys., 22, 6115–6134, https://doi.org/10.5194/acp-22-6115-2022, 2022.

Carn, S. A., Clarisse, L., & Prata, A. J. (2016). Multi-decadal satellite measurements of global volcanic degassing. Journal of Volcanology and Geothermal Research, 311, 99-134.

Carn, S. A., Newman, P. A., Aquila, V., Gonnermann, H., & Dufek, J. (2021). Anticipating climate impacts of major volcanic eruptions. *Eos*, *102*.

Chahine, M., Barnet, C., Olsen, E. T., Chen, L., & Maddy, E. (2005). On the determination of atmospheric minor gases by the method of vanishing partial derivatives with application to CO_2. *Geophysical Research Letters*, *32*(22). https://doi.org/https://doi.org/10.1029/2005GL024165

Clarisse, L., Coheur, P.-F., Theys, N., Hurtmans, D., and Clerbaux, C.: The 2011 Nabro eruption, a SO_2 plume height analysis using IASI measurements, Atmos. Chem. Phys., 14, 3095–3111, https://doi.org/10.5194/acp-14-3095-2014, 2014.

de Leeuw, J., Schmidt, A., Witham, C. S., Theys, N., Taylor, I. A., Grainger, R. G., Pope, R. J., Haywood, J., Osborne, M., & Kristiansen, N. I. (2021). The 2019 Raikoke volcanic eruption -- Part 1: Dispersion model simulations and satellite retrievals of volcanic sulfur dioxide. *Atmospheric Chemistry and Physics*, *21*(14), 10851–10879. https://doi.org/10.5194/acp-21-10851-2021

Fairlie, T. D., Vernier, J.-P., Natarajan, M., & Bedka, K. M. (2014). Dispersion of the Nabro volcanic plume and its relation to the Asian summer monsoon. *Atmospheric Chemistry and Physics*, *14*(13). https://doi.org/10.5194/acp-14-7045-2014

Firstov, P. P., Popov, O. E., Lobacheva, M. A., Budilov, D. I., & Akbashev, R. R. (2020). *Wave perturbations in the atmosphere accompanied the eruption of the Raykoke volcano (Kuril Islands) 21--22 June, 2019*.

Folch, A., Costa, A., and Macedonio, G.: FPLUME-1.0: An integral volcanic plume model accounting for ash aggregation, Geosci. Model. Dev., 9, 431–450, https://doi.org/10.5194/gmd9-431-2016, 2016.

Fromm, M., Nedoluha, G., & Charvát, Z. (2013). Comment on “Large Volcanic Aerosol Load in the Stratosphere Linked to Asian Monsoon Transport.” *Science*, *339*(6120), 647. https://doi.org/10.1126/science.1228605

Hedelt, P., Efremenko, D. S., Loyola, D. G., Spurr, R., and Clarisse, L.: Sulfur dioxide layer height retrieval from Sentinel-5 Precursor/TROPOMI using FP_ILM, Atmos. Meas. Tech., 12, 5503–5517, https://doi.org/10.5194/amt-12-5503-2019, 2019

Gorkavyi, N., Krotkov, N., Li, C., Lait, L., Colarco, P., Carn, S., DeLand, M., Newman, P., Schoeberl, M., Taha, G., Torres, O., Vasilkov, A., & Joiner, J. (2021). Tracking aerosols and SO_2 clouds from the Raikoke eruption: 3D view from satellite observations. *Atmospheric Measurement Techniques*, *14*(12), 7545–7563. https://doi.org/10.5194/amt-14-7545-2021

Gorshkov G S, 1970, Volcanism and the Upper Mantle; Investigations in the Kurile Island Arc, New York: Plenum Publishing Corp, 385 p.

Harvey, N. J., Dacre, H. F., Saint, C., Prata, A. T., Webster, H. N., and Grainger, R. G.: Quantifying the impact of meteorological uncertainty on emission estimates and the risk to aviation using source inversion for the Raikoke 2019 eruption, Atmos. Chem. Phys., 22, 8529–8545, https://doi.org/10.5194/acp-22-8529-2022, 2022.

Horváth, Á., Carr, J. L., Girina, O. A., Wu, D. L., Bril, A. A., Mazurov, A. A., Melnikov, D. V., Hoshyaripour, G. A., and Buehler, S. A.: Geometric estimation of volcanic eruption column height from GOES-R near-limb imagery – Part 1: Methodology, Atmos. Chem. Phys., 21, 12189–12206, https://doi.org/10.5194/acp-21-12189-2021, 2021a.

Horváth, Á., Girina, O. A., Carr, J. L., Wu, D. L., Bril, A. A., Mazurov, A. A., Melnikov, D. V, Hoshyaripour, G. A., & Buehler, S. A. (2021). Geometric estimation of volcanic eruption column height from GOES-R near-limb imagery -- Part 2: Case studies. *Atmospheric Chemistry and Physics*, *21*(16), 12207–12226. https://doi.org/10.5194/acp-21-12207-2021b

Hyman, D. M. and Pavolonis, M. J.: Probabilistic retrieval of volcanic SO_2 layer height and partial column density using the Cross-track Infrared Sounder (CrIS), Atmospheric Measurement Techniques, 13, 5891–5921, https://doi.org/10.5194/amt-13-5891-2020, 2020.

Inness, A., Ades, M., Balis, D., Efremenko, D., Flemming, J., Hedelt, P., Koukouli, M.-E., Loyola, D., and Ribas, R.: Evaluating the assimilation of S5P/TROPOMI near real-time SO_2 columns and layer height data into the CAMS integrated forecasting system (CY47R1), based on a case study of the 2019 Raikoke eruption, Geosci. Model Dev., 15, 971–994, https://doi.org/10.5194/gmd-15-971-2022, 2022.

Jensen, E. J., Woods, S., Lawson, R. P., Bui, T. P., Pfister, L., Thornberry, T. D., Rollins, A. W., Vernier, J.-P., Pan, L. L., Honomichl, S., & Toon, O. B. (2018). Ash Particles Detected in the Tropical Lower Stratosphere. *Geophysical Research Letters*, *45*(20). https://doi.org/10.1029/2018GL079605.

Khaykin, S.M., de Laat, A.T.J., Godin-Beekmann, S. *et al.* Unexpected self-lofting and dynamical confinement of volcanic plumes: the Raikoke 2019 case. *Sci Rep* **12**, 22409 (2022). https://doi.org/10.1038/s41598-022-27021-0

Kloss, C., Berthet, G., Sellitto, P., Ploeger, F., Taha, G., Tidiga, M., Eremenko, M., Bossolasco, A., Jégou, F., Renard, J.-B., & Legras, B. (2021). Stratospheric aerosol layer perturbation caused by the 2019 Raikoke and Ulawun eruptions and their radiative forcing. *Atmospheric Chemistry and Physics*, *21*(1), 535–560.

https://doi.org/10.5194/acp-21-535-2021

Knepp, T. N., Thomason, L., Kovilakam, M., Tackett, J., Kar, J., Damadeo, R., and Flittner, D.: Identification of smoke and sulfuric acid aerosol in SAGE III/ISS extinction spectra, Atmos. Meas. Tech., 15, 5235–5260, https://doi.org/10.5194/amt-15-5235-2022, 2022.

Kovilakam, M., Thomason, L. W., Ernest, N., Rieger, L., Bourassa, A., & Millán, L. (2020). The Global Space-based Stratospheric Aerosol Climatology (version 2.0): 1979--2018. *Earth System Science Data*, *12*(4), 2607–2634. https://doi.org/10.5194/essd-12-2607-2020

LeGrande, A., Tsigaridis, K. & Bauer, S. Role of atmospheric chemistry in the climate impacts of stratospheric volcanic injections. Nature Geosci 9, 652–655 (2016). https://doi.org/10.1038/ngeo2771

Marshall, L., Johnson, J. S., Mann, G. W., Lee, L., Dhomse, S. S., Regayre, L., et al. (2019). Exploring how eruption source parameters affect volcanic radiative forcing using statistical emulation. Journal of Geophysical Research: Atmospheres, 124, 964– 985. https://doi.org/10.1029/2018JD028675

Marshall, L. R., Smith, C. J., Forster, P. M., Aubry, T. J., Andrews, T., & Schmidt, A. (2020). Large variations in volcanic aerosol forcing efficiency due to eruption source parameters and rapid adjustments. *Geophysical Research Letters*, 47, e2020GL090241. https://doi.org/10.1029/2020GL090241

Mastin, L. G.: A user-friendly one-dimensional model for wet volcanic plumes, Geochem. Geophy. Geosy., 8, https://doi.org/10.1029/2006GC001455, 2007.

McKeen, S.A., Liu, S.C. and Kiang, C.S., 1984. On the chemistry of stratospheric SO_2 from volcanic eruptions. Journal of Geophysical Research: Atmospheres, 89(D3), pp.4873-4881.

Mills, M. J., et al. (2016), Global volcanic aerosol properties derived from emissions, 1990–2014, using CESM1(WACCM), J. Geophys. Res. Atmos., 121, 2332–2348, doi:10.1002/2015JD024290.

Millán, L., Santee, M. L., Lambert, A., Livesey, N. J., Werner, F., Schwartz, M. J., et al. (2022). The Hunga Tonga-Hunga Ha'apai Hydration of the Stratosphere. *Geophysical Research Letters*, 49, e2022GL099381. https://doi.org/10.1029/2022GL099381

Mingari, L., Folch, A., Prata, A. T., Pardini, F., Macedonio, G., and Costa, A.: Data assimilation of volcanic aerosol observations using FALL3D+PDAF, Atmos. Chem. Phys., 22, 1773–1792, https://doi.org/10.5194/acp-22-1773-2022, 2022.

Field Code Changed

Müller, W. A., Jungclaus, J. H., Mauritsen, T., Baehr, J., Bittner, M., Budich, R., et al. (2018). A higher-resolution version of the Max Planck Institute Earth System Model (MPI-ESM1.2-HR). Journal of Advances in Modeling Earth Systems, 10, 1383– 1413. https://doi.org/10.1029/2017MS001217

Muser, L. O., Hoshyaripour, G. A., Bruckert, J., Horváth, Á., Malinina, E., Wallis, S., Prata, F. J., Rozanov, A., von Savigny, C., Vogel, H., & Vogel, B. (2020). Particle aging and aerosol-radiation interaction affect volcanic plume dispersion: evidence from the Raikoke 2019 eruption. *Atmospheric Chemistry and Physics*, *20*(23), 15015–15036. https://doi.org/10.5194/acp-20-15015-2020

Osborne, M. J., de Leeuw, J., Witham, C., Schmidt, A., Beckett, F., Kristiansen, N., Buxmann, J., Saint, C., Welton, E. J., Fochesatto, J., Gomes, A. R., Bundke, U., Petzold, A., Marenco, F., & Haywood, J. (2022). The 2019 Raikoke volcanic eruption - Part 2: Particle-phase dispersion and concurrent wildfire smoke emissions. *Atmospheric Chemistry and Physics*, *22*(5), 2975–2997. https://doi.org/10.5194/acp-22-2975-2022

Petracca, I., De Santis, D., Picchiani, M., Corradini, S., Guerrieri, L., Prata, F., Merucci, L., Stelitano, D., Del Frate, F., Salvucci, G., and Schiavon, G.: Volcanic cloud detection using Sentinel-3 satellite data by means of neural networks: the Raikoke 2019 eruption test case, Atmos. Meas. Tech., 15, 7195–7210, https://doi.org/10.5194/amt-15-7195-2022, 2022.

Prata, A. J., & Bernardo, C. (2007). Retrieval of volcanic SO_2 column abundance from Atmospheric Infrared Sounder data. *Journal of Geophysical Research: Atmospheres*, *112*(D20). https://doi.org/https://doi.org/10.1029/2006JD007955

Prata, A. T., Mingari, L., Folch, A., Macedonio, G., and Costa, A.: FALL3D-8.0: a computational model for atmospheric transport and deposition of particles, aerosols and radionuclides – Part 2: Model validation, Geosci. Model Dev., 14, 409–436, https://doi.org/10.5194/gmd-14-409-2021, 2021.

Prata, A. T., Grainger, R. G., Taylor, I. A., Povey, A. C., Proud, S. R., and Poulsen, C. A.: Uncertainty-bounded estimates of ash cloud properties using the ORAC algorithm: application to the 2019 Raikoke eruption, Atmos. Meas. Tech., 15, 5985–6010, https://doi.org/10.5194/amt-15-5985-2022, 2022.

Sawamura, P., Vernier, J. P., Barnes, J. E., Berkoff, T. A., Welton, E. J., Alados-Arboledas, L., Navas-Guzmán, F., Pappalardo, G., Mona, L., Madonna, F., Lange, D., Sicard, M., Godin-Beekmann, S., Payen, G., Wang, Z., Hu, S., Tripathi, S. N., Cordoba-Jabonero, C., & Hoff, R. M. (2012). Stratospheric AOD after the 2011

Formatted: Indent: Left: 0", First line: 0"

Field Code Changed

eruption of Nabro volcano measured by lidars over the Northern Hemisphere. *Environmental Research Letters*, *7*(3). https://doi.org/10.1088/1748-9326/7/3/034013

Sellitto, P., Podglajen, A., Belhadji, R., Boichu, M., Carboni, E., Cuesta, J., Duchamp, C., Kloss, C., Siddans, R., Bègue, N., Blarel, L., Jegou, F., Khaykin, S., Renard, J.-B., & Legras, B. (2022). The unexpected radiative impact of the Hunga Tonga eruption of 15th January 2022. *Communications Earth & Environment*, *3*(1), 288. https://doi.org/10.1038/s43247-022-00618-z

Sennert, 2019. Global Volcanism Program, 2019. Report on Raikoke (Russia). Weekly Volcanic Activity Report, 26 June-2 July 2019. Smithsonian Institution and US Geological Survey.

Schmidt, A., et al. (2018). Volcanic radiative forcing from 1979 to 2015. Journal of Geophysical Research: Atmospheres, 123(22), 12491-12508.

Schmidt, A., Aubry, T.J., Rigby, R., Stevenson, J. and Loughlin, S., Volc2Clim online tool, 2023, https://doi.org/10.5281/zenodo.7602062, https://volc2clim.bgs.ac.uk/.

Smith, C. J., Forster, P. M., Allen, M., Leach, N., Millar, R. J., Passerello, G. A., & Regayre, L. A. (2018). FAIR v1.3: a simple emissions-based impulse response and carbon cycle model. *Geoscientific Model Development*, *11*(6), 2273–2297. https://doi.org/10.5194/gmd-11-2273-2018

Stenchikov, G., Ukhov, A., Osipov, S., Ahmadov, R., Grell, G., Cady-Pereira, K., et al. (2021). How does a Pinatubo-size volcanic cloud reach the middle stratosphere? Journal of Geophysical Research: Atmospheres, 126, e2020JD033829. https://doi.org/10.1029/2020JD033829

Tackett, J. L., Winker, D. M., Getzewich, B. J., Vaughan, M. A., Young, S. A., and Kar, J.: CALIPSO lidar level 3 aerosol profile product: version 3 algorithm design, Atmos. Meas. Tech., 11, 4129–4152, https://doi.org/10.5194/amt-11-4129-2018, 2018.

Theys, N., Campion, R., Clarisse, L., Brenot, H., van Gent, J., Dils, B., Corradini, S., Merucci, L., Coheur, P.-F., Van Roozendael, M., Hurtmans, D., Clerbaux, C., Tait, S., & Ferrucci, F. (2013). Volcanic SO_2 fluxes derived from satellite data: a survey using OMI, GOME-2, IASI and MODIS. *Atmospheric Chemistry and Physics*, *13*(12), 5945–5968. https://doi.org/10.5194/acp-13-5945-2013

Theys, N., De Smedt, I., Yu, H., Danckaert, T., van Gent, J., Hörmann, C., Wagner, T., Hedelt, P., Bauer, H., Romahn, F., Pedergnana, M., Loyola, D., & Van Roozendael, M. (2017). Sulfur dioxide retrievals from TROPOMI onboard Sentinel-5 Precursor: algorithm theoretical basis. *Atmospheric Measurement Techniques*, *10*(1), 119–153. https://doi.org/10.5194/amt-10-119-2017

Field Code Changed

Formatted: Font: (Default) Times New Roman, 10 pt, English (United States)

Formatted: Font: (Default) Times New Roman, 10 pt

Formatted: Font: (Default) Times New Roman, 10 pt, English (United States)

Theys, N., Fioletov, V., Li, C., De Smedt, I., Lerot, C., McLinden, C., Krotkov, N., Griffin, D., Clarisse, L., Hedelt, P., Loyola, D., Wagner, T., Kumar, V., Innes, A., Ribas, R., Hendrick, F., Vlietinck, J., Brenot, H., & Van Roozendael, M. (2021). A sulfur dioxide Covariance-Based Retrieval Algorithm (COBRA): application to TROPOMI reveals new emission sources. *Atmospheric Chemistry and Physics*, *21*(22), 16727–16744. https://doi.org/10.5194/acp-21-16727-2021

Theys, N., Lerot, C., Brenot, H., van Gent, J., De Smedt, I., Clarisse, L., Burton, M., Varnam, M., Hayer, C., Esse, B., & Van Roozendael, M. (2022). Improved retrieval of SO_2 plume height from TROPOMI using an iterative Covariance-Based Retrieval Algorithm. *Atmospheric Measurement Techniques*, *15*(16), 4801–4817. https://doi.org/10.5194/amt-15-4801-2022

Tournigand, P.-Y., Cigala, V., Lasota, E., Hammouti, M., Clarisse, L., Brenot, H., Prata, F., Kirchengast, G., Steiner, A. K., & Biondi, R. (2020). A multi-sensor satellite-based archive of the largest SO_2 volcanic eruptions since 2006. *Earth System Science Data*, *12*(4), 3139–3159. https://doi.org/10.5194/essd-12-3139-2020

Vaughan, G., Wareing, D., and Ricketts, H.: Measurement Report: Lidar measurements of stratospheric aerosol following the 2019 Raikoke and Ulawun volcanic eruptions, Atmos. Chem. Phys., 21, 5597–5604, https://doi.org/10.5194/acp-21-5597-2021, 2021.

Veefkind, J. P., Aben, I., McMullan, K., Förster, H., de Vries, J., Otter, G., Claas, J., Eskes, H. J., de Haan, J. F., Kleipool, Q., van Weele, M., Hasekamp, O., Hoogeveen, R., Landgraf, J., Snel, R., Tol, P., Ingmann, P., Voors, R., Kruizinga, B., … Levelt, P. F. (2012). TROPOMI on the ESA Sentinel-5 Precursor: A GMES mission for global observations of the atmospheric composition for climate, air quality and ozone layer applications. *Remote Sensing of Environment*, *120*, 70–83. https://doi.org/https://doi.org/10.1016/j.rse.2011.09.027

Vernier, J.-P., Fairlie, T. D., Deshler, T., Natarajan, M., Knepp, T., Foster, K., Wienhold, F. G., Bedka, K. M., Thomason, L., & Trepte, C. (2016). In situ and space-based observations of the Kelud volcanic plume: The persistence of ash in the lower stratosphere. *Journal of Geophysical Research*, *121*(18). https://doi.org/10.1002/2016JD025344

Vernier, J.-P., Fairlie, T. D., Murray, J. J., Tupper, A., Trepte, C., Winker, D., Pelon, J., Garnier, A., Jumelet, J., Pavolonis, M., Omar, A. H., & Powell, K. A. (2013). An advanced system to monitor the 3D structure of diffuse volcanic ash clouds. *Journal of Applied Meteorology and Climatology*, *52*(9). https://doi.org/10.1175/JAMC-D-12-0279.1

Vömel H, Evan S, Tully M. Water vapor injection into the stratosphere by Hunga Tonga-Hunga Ha'apai. Science. 2022 Sep 23;377(6613):1444-1447. doi: 10.1126/science.abq2299. Epub 2022 Sep 22. PMID: 36137033.

Winker, D. M., Tackett, J. L., Getzewich, B. J., Liu, Z., Vaughan, M. A., & Rogers, R. R. (2013). The global 3-D distribution of tropospheric aerosols as characterized by CALIOP. *Atmospheric Chemistry and Physics*, *13*(6), 3345–3361. https://doi.org/10.5194/acp-13-3345-2013

Winker, D. M., Pelon, J., Coakley, J. A., Ackerman, S. A., Charlson, R. J., Colarco, P. R., Flamant, P., Fu, Q., Hoff, R. M., Kittaka, C., Kubar, T. L., Le Treut, H., Mccormick, M. P., Mégie, G., Poole, L., Powell, K., Trepte, C., Vaughan, M. A., & Wielicki, B. A. (2010). The CALIPSO Mission. *Bulletin of the American Meteorological Society*, *91*(9), 1211–1230. https://doi.org/10.1175/2010BAMS3009.1

Wrana, F., Niemeier, U., Thomason, L. W., Wallis, S., and von Savigny, C.: Stratospheric aerosol size reduction after volcanic eruptions, Atmos. Chem. Phys., 23, 9725–9743, https://doi.org/10.5194/acp-23-9725-2023, 2023.

Zängl, G., Reinert, D., Rípodas, P., and Baldauf, M.: The ICON (ICOsahedral Non-hydrostatic) modelling framework of DWD and MPI-M: Description of the non-hydrostatic dynamical core, Q. J. Roy. Meteor. Soc., 141, 563–579, https://doi.org/10.1002/qj.2378, 2015. a, b, c

Zhu, Y., Toon, O.B., Jensen, E.J. et al. Persisting volcanic ash particles impact stratospheric SO_2 lifetime and aerosol optical properties. Nat Commun 11, 4526 (2020). https://doi.org/10.1038/s41467-020-18352-5

Figures.

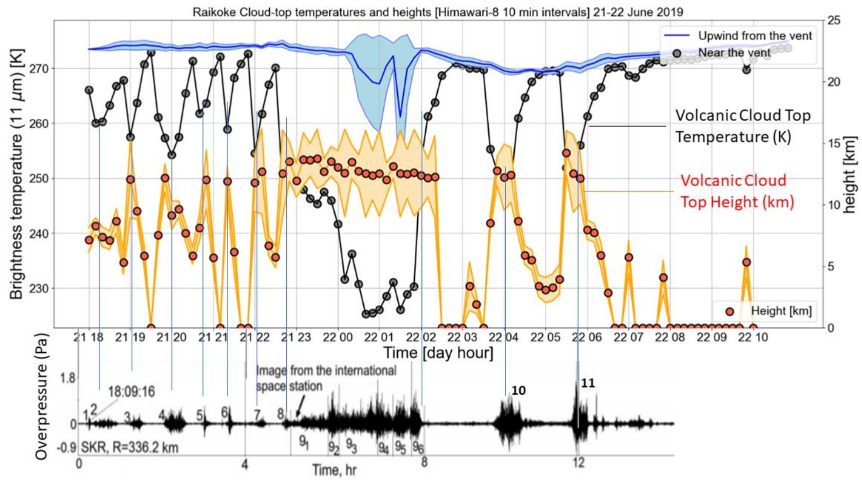

Figure 1. (Top) Time series of Himawari-8 cloud-top brightness temperatures from the 11 micron channel. The blue line corresponds to the mean of 3x3 pixels at a point upwind, but close to, the vent. The shaded region represents ±1 sigma from the mean. The grey dots are brightness temperatures at the pixel closest to the vent. The brightness temperature (BT) rapid decreases at the vent, that are not coincident with the upwind values, suggest eruptive columns with cold, high cloud tops. The BT values should be read from the left-hand ordinate axis. The orange dots with uncertainties (shaded) correspond to cloud-top heights (right-hand ordinate axis) taken from Prata et al. (2022) Modified from Fig.7 from (Firstov et al., 2020) showing IS signals during the first 12h after the beginning of the Raikoke eruption which started near 18 UTC on June 21 2019. (Bottom) A time series of corresponding Brightness Cloud Top Temperature at 11μm derived from HIMWARI-8 is shown. Height retrievals near the vent (orange data points) and uncertainties (orange shaded region) taken from Prata et al. (2022).(Bottom) Modified from Fig.7 from (Firstov et al., 2020) showing ISInfraSound (IS) signals (overpressure) during the first 12h after the beginning of the Raikoke eruption which started near 17:53:5418 UTC on June 21 2019 from a ground station on Paramushir Island (SKR, southern tip of Kamchatka). The numbers indicate the separate episodes of the eruption, defined by the records at SKR. The blue lines connect those IS episodes with observed minimum in cloud top temperature. R corresponds to the distance between the station and the Raikoke volcano.. (Bottom)

Formatted: Font: (Default) Times New Roman, Bold, English (United States)

Formatted: Font: Bold, English (United States)

Formatted: Font: (Default) Times New Roman, 10 pt, Bold, English (United States)

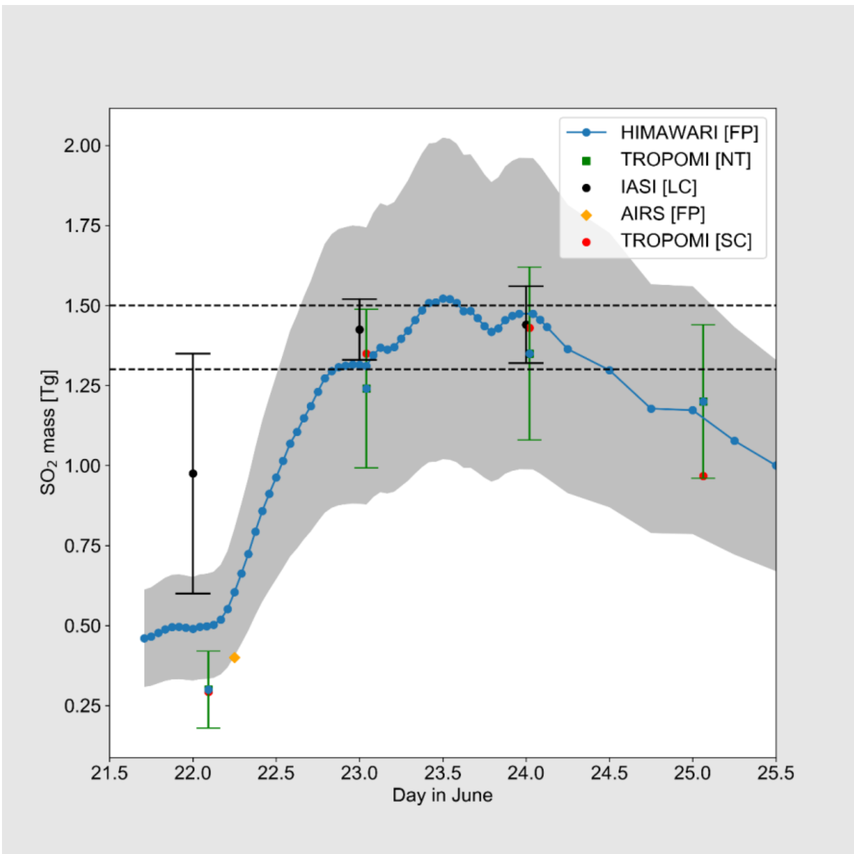

Figure 2. Total SO_2 mass (Tg) as a function of time in June 2019 estimated from various satellite sensors for the eruption of Raikoke. The grey-colored region indicates the uncertainty range of the Himawari-8 (AHI) retrievals. A ±20% uncertainty has been placed on the TROPOMI estimates. The IASI estimates come from different satellites and times of day (day/night); the vertical lines on these data indicate the range of the estimations. Himawari-8 samples every 10 minutes. After 24 June retrievals were performed at longer intervals. Distributed to VolRes on 06/28/2019.

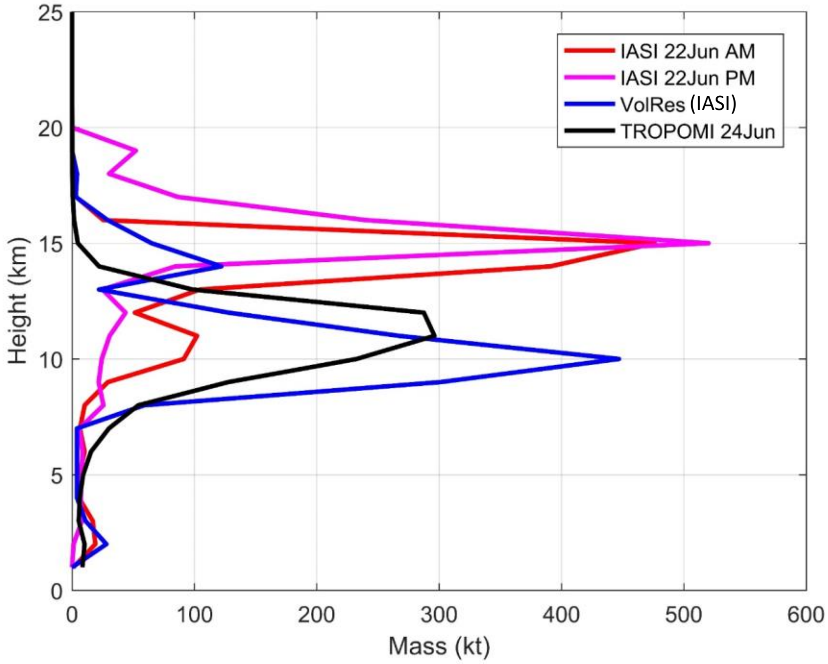

Figure 3: SO_2 **mass altitude distribution from IASI (refined analysis), VolRes (IASI initial estimate) and TROPOMI. The associated data is provided in Table 2~~1~~.**

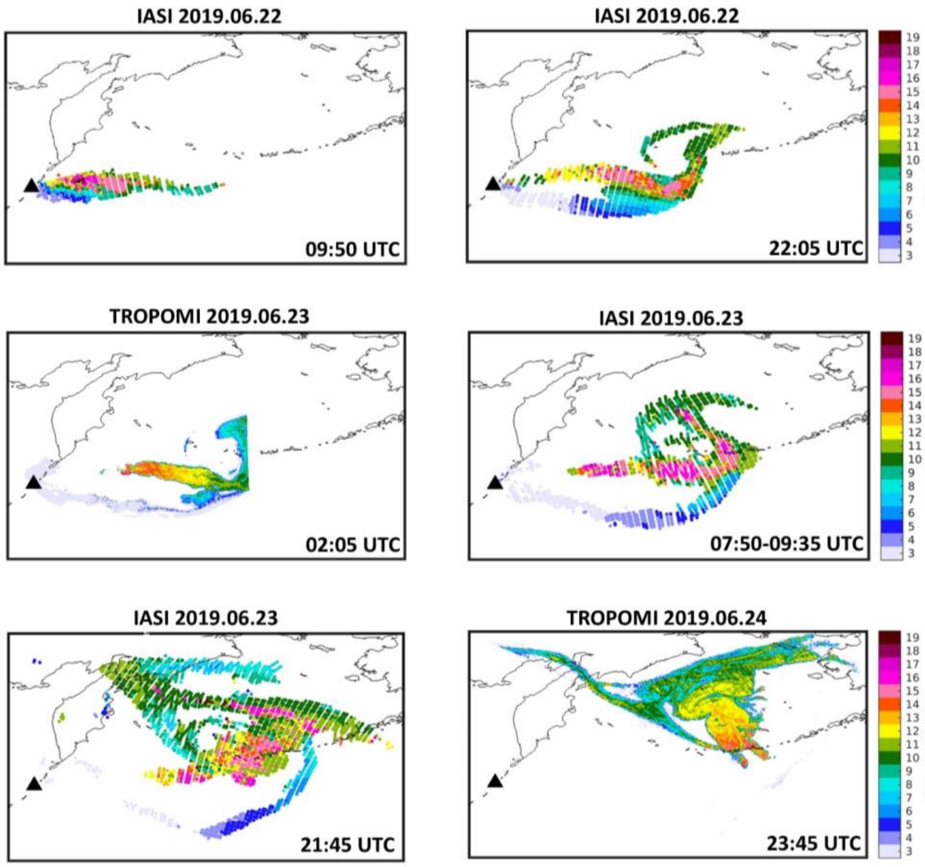

Figure 4: Examples of SO_2 **height retrievals from IASI (refined analysis) and TROPOMI for Raikoke eruption for 22-24 June 2019. The Raikoke volcano is marked by a black triangle. Approximate overpass times are indicated in each panel.**

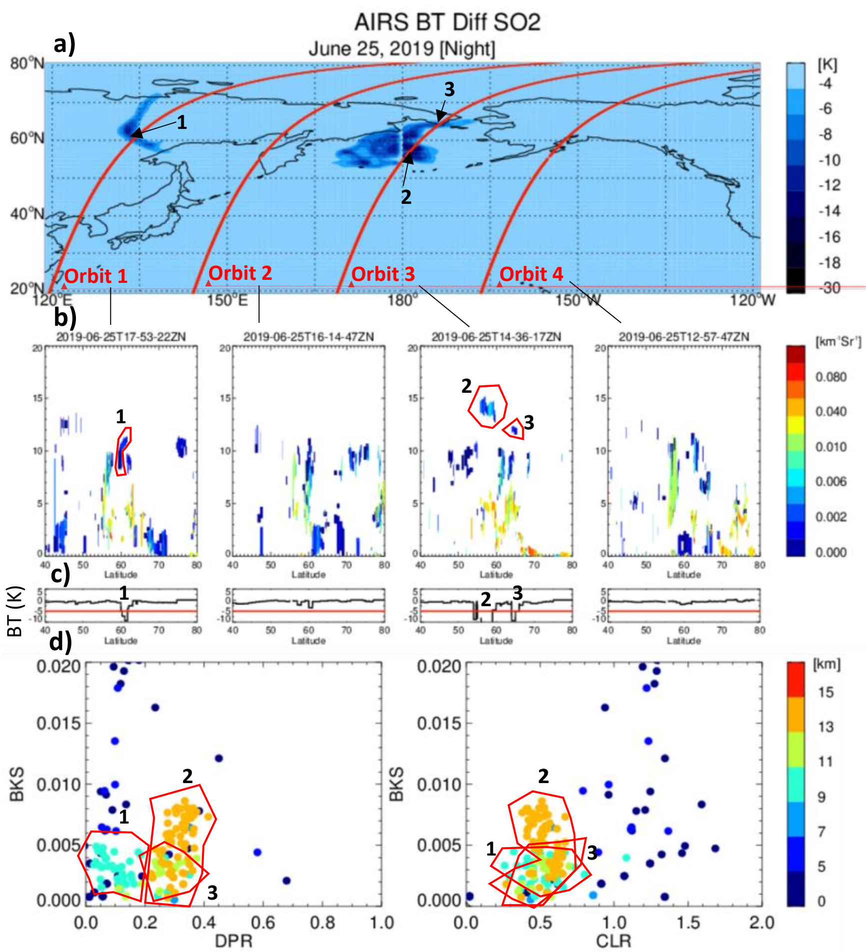

Figure 5. (a) AIRS Nighttime Brightness Temperature Difference (BTD) (1361.44-1433.06 cm^{-1}) on 25 June 2022 together with 4 CALIOP ground-tracks (red). (b) Corresponding aerosol and cloud layer products from CALIOP level 2V4.2 product and (c) extracted AIRS BTD extracted along the CALIOP orbit tracks. The red line correspond to the threshold used for detecting volcanic enhancement (d) diagrams of particular backscatter (BKS) as a function of mean layer particulate DePolarization Ratio (DPR) (left) and particulate CoLor Ratio (CLR) (right) derived from CALIOP and colored by mid-layer altitudes.

Formatted: Font color: Red

Formatted: Font color: Red

Formatted: Font color: Red

Formatted: Font color: Red

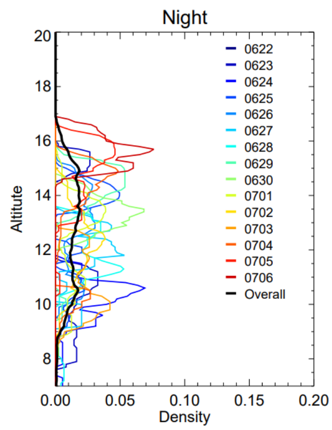

Figure 6. Daily nighttime Probability Density Function profiles of the mid-layer geometric altitude for volcanic layers observed by CALIOP/AIRS using plume identification criterion when DPR < 0.4 and CLR < 0.7 and altitude > 5km and BTD < -6K between 06/22 and 07/06. The black line is the overall pdf profile using all nighttime data between 06/22 and 07/06.

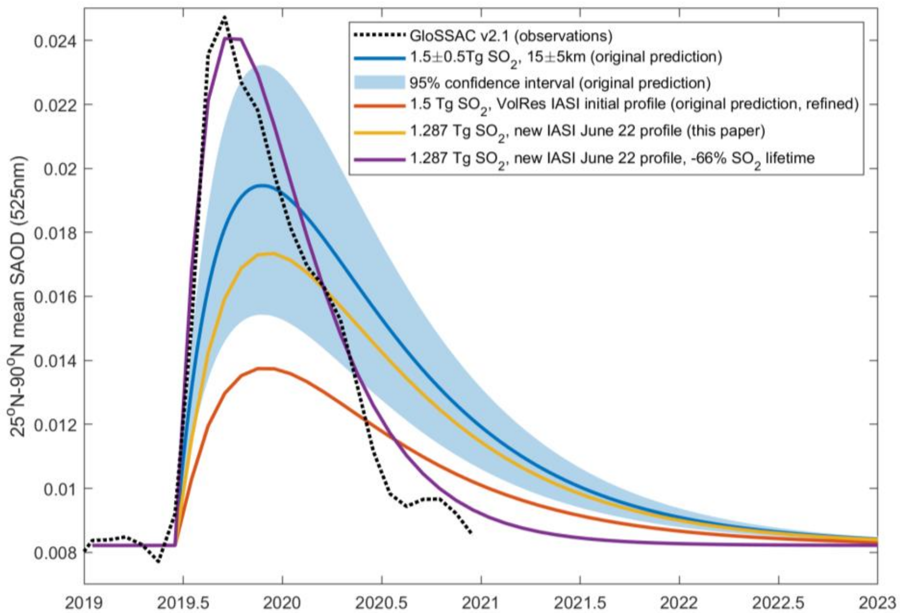

Figure 7: Northern Hemisphere (25ºN-90ºN) monthly-mean SAOD at 525nm as projected by EVA_H (continuous colored lines) and observed (GloSSAC v2.1, black dashed line). The light blue shading and line shows the first projection made at the time of the eruption and its confidence interval based on an injection height of 15+/-5km and SO_2 mass of 1.5+/-0.5 Tg. The orangeyellow line shows the second projection made at the time of the eruption using the VolRes IASI initial profile. The orange yellow line shows a new projection using the new VolRes IASI June 22 profile presented in this study (Figure 3). The violet line uses the same profile, but the SO_2-to-aerosol conversion timescale in EVA_H reduced by 66%.

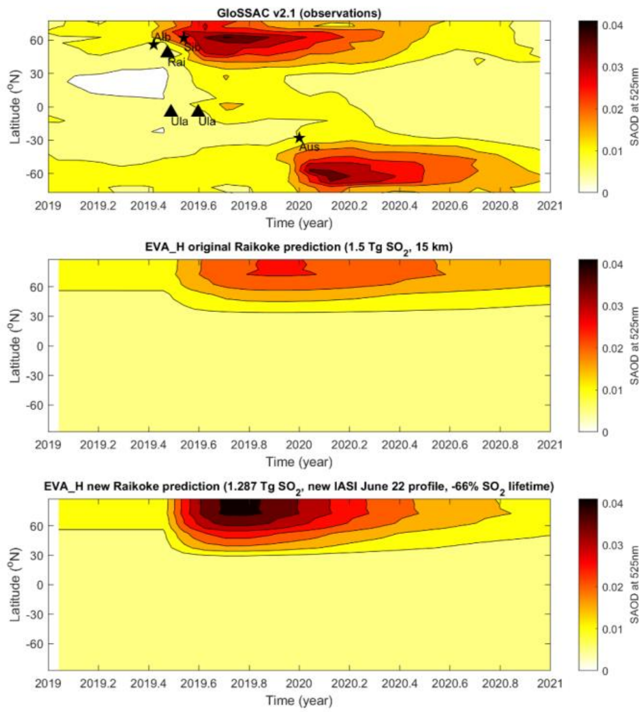

Figure 8: SAOD at 525nm as observed (GloSSAC v2.1, top) and projected by EVA_H following the Raikoke 2019 eruption (middle) and using the revised IASI June 22 SO_2 profile presented in this paper along with the adjusted (-66%) SO_2-to-aerosol conversion timescale in EVA_H (bottom). EVA_H was run only with the Raikoke injections, and not with injections associated with the Ulawun 2019 eruptions (denoted by black triangles in the top panel) nor with wildfire events in Alberta, Siberia (2019) and Australia (2020) (denoted by black stars in the top panel).

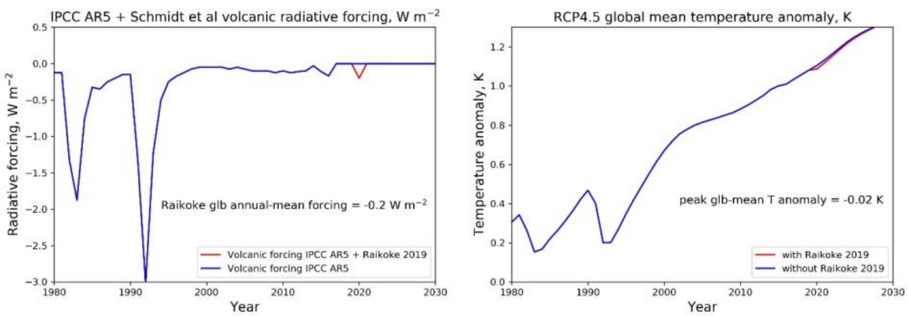

Figure 9: Annual global mean volcanic radiative forcing (left) and corresponding annual global mean surface temperature anomaly calculated using the climate response model FaIR (Smith et al., 2018) (right). Blue and red lines show results with and without accounting for the 2019 Raikoke eruption, respectively. This is the original figure shared on the VolRes mailing list on 06/26/19.

Date	Data type	Activities	Data variables	Platform	Add. Information
06/24	Satellite	SO2 and plume height maps 06/24 & 06/25	SO2 total column (DU) and concentration (ppmv ?)	TROPOMI /Sentinel 5P	Polar Orbit/ESA
06/24	Satellite	Aerosol maps and profiles when ?	Aerosol extinction (km-1)	NPP/OMP S	Polar Orbit/NASA
06/25	Satellite	SO2 maps 06/21 & 06/22	SO2 total column (DU)	Metop/IA SI	Polar Orbit/Eumet sat
06/25	Satellite	Ash and SO2 total column	Ash signature (11-12 um) and SO2 UTLS (VCD DU)	AHI/HIMA WARI-8	Geo Orbit/JAXA
06/25	Satellite	Plume heights and optical properties	Backscatter and depolarization at 532 and 1064 nm	CALIOP/C ALIPSO	Polar Orbit/NASA
06/25	Satellite	Maps of plume height and properties 06/23	Height (km) and AOD, angstrom coeff, SSA	MISR/Terr a	Polar Orbit/NASA
06/25	Model	Volcanic plume maps at 100 and 140 hPa	Aerosol extinction at XX nm	WACCM	Model type
06/25	Model	Impacts on stratospheric aerosol	Stratospheric AOD	GEOS-5	
06/26	Satellite	Mass distribution profile on 06/23	Mass per levels (kt)	TROPOMI/Sentin el 5P	Polar Orbit/ESA
06/26	Satellite	SO2 plume vertical information	SO2 mixing ratio (ppbv)	MLS/Aura	Polar Orbit/ESA
06/26	Model	Radiative and climate impacts	RF TOA (w/m2)	??	
06/28	Model	Trajectory simulation of Raikoke dispersion	Plume height (km)	Langley Trajectory Model	GEOS-5 wind data
07/03	Satellite	Plume height and properties	Backscatter and depolarization at 532 and 1064 nm	CALIOP/CALIPSO	Polar Orbit/ESA
07/09	Model	SO2 and ash plume dispersion 06/21 to 06/25	Ash and SO2 mass concentration	ICONN-ART	
07/10	Ground-based lidar	Vertical plume profiles 07/05	Scattering ratio at 532 nm	OHP/LTA	
07/10	Satellite	Plume height and properties	Backscatter and depolarization at 532 and 1064 nm	CALIOP/CALIPSO	Polar Orbit/NASA
07/10	Satellite	Latitudinal time series	Aerosol extinction (km-1)	NPP/OMPS	NASA
07/16	Satellite	Animation of aerosol maps at 12.5 km, 13.5 km, 14.5 km and 16.5 km across the NH. 06/11 to 07/14	Aerosol extinction (km-1)	OMPS/NP P	Polar Orbit/NASA
07/17	Ground-based lidar	Volcanic aerosol profiles 06/29 and 07/08	RSC 1064 nm	SIRTA	
07/19	Satellite	Maps of SO2 centered in Indonesia/Australia (from 06/26 to 07/12), Ulawun eruption	SO2 DU	TROPOMI /Sentinel 5P	Polar Orbit/ESA
07/20	Satellite	Animation of aerosol maps at 18.5 km from 06/27 to 07/17	Aerosol extinction (km-1) at 674 nm	OMPS/NP P	Polar Orbit/NASA
07/21	Ground-based lidar	Volcanic aerosol profiles on 07/18 and 07/20	Scattering Ratio at 532 nm	OHP LTA	
08/07	Satellite	Animation of aerosol maps at 20.5 km	Aerosol extinction (km-1) at 674 nm	OMPS/NP P	Polar Orbit/NASA
08/24	Satellite	Volcanic plumes cross-section 11-20 Aug 2019	Scattering Ratio at 532 nm	CALIOP/C ALIPSO	Polar Orbit/NASA
09/04	Balloon	Aerosol concentration profiles on 08/26 in Wyoming	Aerosol concentration for r>0.005 um, 0.092, 0.15, 0.28	Balloon	WOPC
09/17	Ground-	Atmospheric profiles of aerosols and	Backscatter profiles at 532 nm	Lidar LOA	

Table 1: VolRes activities during the first 2 months after the Raikoke eruption.

Altitude (km)	**VolRes IASI initial profile**	**IASI 22 June 2019 (AM)**	**IASI 22 June 2019 (PM)**	**TROPOMI 24 June 2019**
1	0	1.1	0	8.4
2	28	19.0	1.2	10.2
3	11	16.9	8	5.4
4	4	5.6	7.1	6.3
5	4	6.0	7.9	9.0
6	4	10.2	8.5	15.5
7	4	6.4	6.0	30.1
8	59	10.3	25.6	54.1
9	301	29.2	21.7	127.6
10	446	91.3	24.2	232.6
11	266	102.1	30.7	296.2
12	128	51.3	43.7	287.5
13	22	104.4	24.8	98.4
14	122	390.9	84.5	22.0
15	65	476.2	520.2	4.7
16	29	25.5	239.7	1.63
17	3	3.3	86.4	0.53
18	4	2.6	30.2	0.19
19	0	0	52.1	0.14
20	0	0	0	0.1
Total	**1500 kt (scaled)**	**1352.3 kt**	**1222.5 kt**	**1210.6 kt**

Table 21: SO_2 **mass profile (in kt) derived from IASI and TROPOMI for the Raikoke eruption.**

Date	Data type	Activities	Data variables	Platform	Add. Information
06/24	Satellite	SO2 and plume height maps 06/24 & 06/25	SO2 total column (DU) and concentration (ppmv ?)	TROPOMI /Sentinel 5P	Polar Orbit/ESA
06/24	Satellite	Aerosol maps and profiles when ?	Aerosol extinction (km-1)	NPP/OMPS	Polar Orbit/NASA
06/25	Satellite	SO2 maps 06/21 & 06/22	SO2 total column (DU)	Metop/IASI	Polar Orbit/Eumetsat
06/25	Satellite	Ash and SO2 total column	Ash signature (11-12 um) and SO2 UTLS (VCD DU)	AHI/HIMAWARI-8	Geo Orbit/JAXA
06/25	Satellite	Plume heights and optical properties	Backscatter and depolarization at 532 and 1064 nm	CALIOP/CALIPSO	Polar Orbit/NASA
06/25	Satellite	Maps of plume height and properties 06/23	Height (km) and AOD, angstrom coeff, SSA	MISR/Terra	Polar Orbit/NASA
06/25	Model	Volcanic plume maps at 100 and 140 hPa	Aerosol extinction at XX nm	WACCM	Model type
06/25	Model	Impacts on stratospheric aerosol	Stratospheric AOD	GEOS-5	
~~07/16~~	~~Satellite~~	~~Animation of aerosol maps at 12.5 km,~~ 13.5 km, 14.5 km and 16.5 km across the NH. 06/11 to 07/14	~~Aerosol extinction~~ (km-1)	OMPS/NPP	Polar Orbit/NASA
07/17	Ground-based lidar	Volcanic aerosol profiles 06/29 and 07/08	RSC 1064 nm	SIRTA	
07/19	Satellite	Maps of SO2 centered in Indonesia/Australia (from 06/26 to 07/12), Ulawun eruption	SO2 DU	TROPOMI /Sentinel 5P	Polar Orbit/ESA
07/20	Satellite	Animation of aerosol maps at 18.5 km from 06/27 to 07/17	Aerosol extinction (km-1) at 674 nm	OMPS/NPP	Polar Orbit/NASA
07/21	Ground-based lidar	Volcanic aerosol profiles on 07/18 and 07/20	Scattering Ratio at 532 nm	OHP LTA	
08/07	Satellite	Animation of aerosol maps at 20.5 km	Aerosol extinction (km-1) at 674 nm	OMPS/NPP	Polar Orbit/NASA
08/24	Satellite	Volcanic plumes cross-section 11-20 Aug 2019	Scattering Ratio at 532 nm	CALIOP/CALIPSO	Polar Orbit/NASA
09/04	Balloon	Aerosol concentration profiles on 08/26 in Wyoming	Aerosol concentration for r>0.005 um, 0.092, 0.15, 0.28	Balloon	WOPC
09/17	Ground-	Atmospheric profiles of aerosols and	Backscatter profiles at 532 nm	Lidar LOA	

~~**Table 2: VolRes activities during the first 2 months after the Raikoke eruption.**~~